ISSN: 2538-2152; ECOPERSIA 2025;13(4): 407-427.

Landslide Susceptibility Assessment using Bivariate and Data Mining Methods

ARTICLEINFO

Article Type
Original Research

Authors
Majid Mohammady, *Ph.D.*[*]

How to cite this article
Mohammady M. Landslide Susceptibility Assessment using Bivariate and Data Mining Methods. ECOPERSIA 2025;13(4): 407-427.
DOI:
10.48311/ECOPERSIA.13.4.407

Associate Professor, College of Natural Resources, Semnan University, Semnan, Iran.

*** *Correspondence***
Address: Associate Professor, College of Natural Resources, Semnan University, Semnan, Iran.
Tel: +98 (23) 3153 3040
Email: majid.mohammady@semnan.ac.ir

Article History
Received: September 26, 2025
Accepted: November 18, 2025
Published: November 26, 2025

ABSTRACT

Aims: The primary objective of the study is to examine the simultaneous use of machine learning with complex modeling processes and to compare their accuracy with that of the frequency ratio method, a simple statistical method, in northern Tehran. Due to its milder climate compared to Tehran City, residential areas and gardens have developed, leading to increased road construction and, in turn, a rise in landslide incidents.

Material & Methods: A landslide distribution map was prepared using Google Earth and field survey data. Twelve factors were selected as conditioning factors. Generalized linear models, multivariate adaptive regression splines, and frequency-ratio models were applied to generate susceptibility maps. The ROC curve was used for model validation. The areas of the susceptibility classes were also calculated for three models.

Findings: The FR and GLM models achieved good accuracy, while the MARS model demonstrated very good accuracy. The areas under the ROC curves were 0.771, 0.767, and 0.822 for the FR, GLM, and MARS models, respectively. The susceptibility classes show that 37%, 44%, and 44% of the study area have high and very high susceptibility in the FR, GLM, and MARS models, respectively.

Conclusion: The calculated susceptibility area indicates that the region is very susceptible to landslides, warranting careful attention in regional planning and development. Geographical datasets and landslide susceptibility maps provide valuable resources for sustainable planning in the area, land-use planning, and identification of vulnerable regions.

Keywords: Capital of Iran; Frequency Ratio; GLM; Machine Learning; MARS; ROC Curve; Susceptibility Mapping.

CITATION LINKS

[1] Fang Z., Wang Y., Peng L., Hong H. Integration of con... [2] Froude M., Petley D. Global fatal landslide occurrenc... [3] Chowdhury S., Rahman N., Sheikh S., Sayeid A., Mahmud... [4] Iranian Landslide Working Party (ILWP) (2007). Irania... [5] Shoaei Z., Ghayoumian J. Toward the Mechanism of Dead... [6] Hadian Amri M., Solaimani K., Kavian A., Afzal P. A n... [7] Liu X.D., Xiao T., Zhang S.H., Sun P.H., Liu L.L., Pe... [8] Youssef K., Shao K., Moon S., Bouchard L.S. Landslide... [9] Rai S.C., Pandey V.K., Sharma K.K., Sharma S. Landsli... [10] Khan H., Shafique M., Khan M.A., Bacha M.A., Shah S.U... [11] Mohammady M., Pourghasemi H.R., Pradhan B. Landslide ... [12] Alsabhan A.H., Singh K., Sharma A., Alam S., Pandey D... [13] Asmare D., Application and validation of AHP and FR m... [14] Li M., Wang H., Chen J., Zheng K. Assessing landslide... [15] Zhang W., Liu S., Wang L., Samui P., Chwała M., He Y.... [16] Guo Z., Guo F., Zhang U., He J., Li G., Yang Y., Zhan... [17] 17. Zhang A., Zhao X.W., Zhao X.Y., Zheng X.Z., Zeng ... [18] Ahmad M.S., Lisa M., Khan S. Comparative analysis of ... [19] Yuvaraj R.M., Dolui B. Geographical assessment of lan... [20] Bisht S., Rawat K.S., Singh S.K. Earth observation da... [21] Geology Survey of Iran (GSI). 1997; https://gsi.ir/en... [22] Sevgen E., Kocaman S., Nefeslioglu H.A., Gokceoglu C.... [23] Zakerinejad R., Maerker M. An integrated assessment o... [24] Zeng T., Wu L., Peduto D., Glade T., Hayakawa Y.S., Y... [25] Dai F.C., Lee C.F., Li J.X.Z.W., Xu Z.W. Assessment o... [26] O'Brien R.M. A caution regarding rules of thumb for v... [27] Atkinson P., Jiskoot H., Massari R., Murray T. Genera... [28] Mohammady M., Davudirad A. Gully Erosion Susceptibili... [29] Nordin N.D., Zan M.S.D., Abdullah F. Generalized line... [30] Felicísimo Á.M., Cuartero A., Remondo J., Quirós E. M... [31] Chu L., Wang L.J., Jiang J., Liu X., Sawada K., Zhang... [32] Mohammady M., Pourghasemi H.R., Amiri M., Tiefenbache... [33] Dhakal D., Singh K. A Geospatial Approach to Landslid... [34] Yesilnacar E.K. The application of computational inte... [35] Mosaffaie J., Salehpour Jam A., Sarfaraz F. Landslide... [36] Pourghasemi H.R., Mohammady M., Pradhan B. Landslide ... [37] Hong H. Assessing landslide susceptibility based on h... [38] Hunter G., Fell R. Travel distance angle for "rapid" ... ... [39] Donati L., Turrini M.C. An objective method to rank t... [40] Roback K., Clark M.K., West A.J., Zekkos D., Li G., G... [41] Kisi O., Parmar K. Application of least square suppor... [42] Zheng G., Yang P., Zhou H., Zeng C., Yang X., He X., ... [43] Mohammady M. Badland erosion susceptibility mapping u... [44] Dlamini, W.M. Analysis of deforestation patterns and ... [45] Mosaffaie J., Salehpour Jam A., Tabatabaei M.R. Compa... [46] Salehpour Jam A., Mosaffaie J., Sarfaraz F., Shadfar ... [47] Salehpour Jam A., Mosaffaie J., Tabatabaei M.R. Raste...

Introduction

Landslides cause enormous losses of ecological resources, property, and human life. In mountainous regions, mass movement and landslides represent major erosional processes. Large volumes of soil and sediment can enter the river system through landslides, causing debris flows in mountainous areas [1]. Infrastructure damage is caused by the transportation of soil and rocks by landslides along the slope (breakdown of the gas, water, and sewage systems, settlement, and communication lines). From January 2004 to December 2016, an average of 400 fatal landslides occurred annually, resulting in 55,997 deaths worldwide [2]. Human activities cause most fatal landslides, and their frequency has been steadily increasing over time [2]. Landslides account for about 5.08% of all global environmental disasters, with nearly 53.88% of events occurring in Asia [3]. Due to its geological conditions, soil characteristics, and poor land management, Iran is highly susceptible to landslides. According to reports in Iran, 187 people were killed in landslide events, and many infrastructures, including 252.67 km of main roads, 6 km of railroads, 3 km of forest roads, and 46 km of rural roads, were damaged between 1982 and 2007. Until 2007, the estimated damage from mass movements, particularly landslides, was 126893 billion Rials in Iran [4]. For example, a landslide in Farsan City, Iran (April 1, 1998), resulted in 54 deaths, destroyed 40 hectares of farmland, and caused the loss of 1,300 livestock [5].

Watershed management relies heavily on zonation of landslide-prone areas, which are critical for assessing environmental threats. Landslide susceptibility maps are helpful because they continuously display the spatial probability of landslides based on the influencing factors. A susceptibility map shows which regions are susceptible to future landslides by simulating landslide probabilities, thereby providing more references for landslide hazard assessments [6, 7]. The most effective strategies for reducing landslide hazards are appropriate monitoring, accurate assessment, and identification of landslide-vulnerable areas. Policymaking and management in the area utilize landslide susceptibility maps. Because landslide occurrence is controlled by complex interactions among factors such as tectonics, hydrology, vegetation, geology, precipitation, temperature, and erosion, reliable analytical methods are essential for assessing slope instability.

It is challenging to determine historical landslide locations, and the processes that cause landslides are complex and ambiguous; consequently, assessing landslide susceptibility remains difficult [8]. Although landslide-sensitive areas have been mapped using various methods, no single method has proven entirely suitable. The performance of a model varies by location, and its efficacy differs across regions. For a specific study area, the error rates of several methods are compared to overcome this restriction, and the optimal model is the one that achieves the highest accuracy [3]. Advances in Geographic Information Systems (GIS) and remote sensing techniques have facilitated the integration of spatial and non-spatial datasets, enabling more robust landslide susceptibility analyses at multiple scales [9].

There are various techniques for landslide susceptibility analysis, such as qualitative, physical, quantitative, and semi-quantitative models. Statistical and machine learning

techniques are particularly effective for quantitatively analyzing the bivariate and multivariate correlations between landslides and effective factors. These methods estimate the probability of landslide occurrence based on a landslide distribution map. Machine learning approaches are more accurate and yield better outcomes than other quantitative models [3]. Numerous studies have examined landslide susceptibility using a range of qualitative and quantitative methods. Some of these models are frequency ratios [10], weight of evidence [11, 12], information value [12], logistic regression [3], fractal models [6], expert-knowledge-based models, such as the analytical hierarchy process [13], and many machine learning techniques. In this study, a simple bivariate statistical model (Frequency Ratio) and two more complex machine learning models (Generalized linear model and multivariate adaptive regression spline) were applied to produce a landslide susceptibility map.

Many studies have utilized machine learning for landslide susceptibility assessment in various regions. In this context, Li et al. [14] used a random forest to create landslide susceptibility in Henan Province, China. Zhang et al. [15] used a class-weighted method, an integrated machine learning model (LightGBM and random forests), and conventional machine learning (logistic regression) to examine landslide susceptibility in Yunyang County, Chongqing, China. Guo et al. [16] used four data-mining techniques for landslide susceptibility assessment. These findings indicate that data-mining techniques are accurate models in Lantian County, China. Zhang et al. [17] used SVM, RF, logistic regression, and gradient boosting for landslide susceptibility analysis in the Conghua, China. Rai et al. [9] applied several machine-learning models to assess landslides in India.

A statistical model of the frequency ratio has also been widely used. For example, Asmare [13] applied frequency ratio and AHP models for landslides assessment in Choke Mountain, NW Ethiopia. Ahmad et al. [18] used frequency ratio and AHP to assess the landslide susceptibility in a part of Pakistan. The finding revealed that the frequency ratio is better than the AHP. Yuvaraj and Dolui [19] and Bisht et al. [20] used the frequency ratio model to map landslide susceptibility in India.

The Tehran metropolitan area lies within the Alborz Mountains and is bounded by the Mosha, North Tehran, and Taleghan faults. The development of the Tehran residential area on the steep slopes of the North Tehran Fault has increased the risk of disasters, including floods, earthquakes, severe erosion, and landslides. The presence of geological formations such as marl, sandstone, shale, claystone, and siltstone, along with sufficient rainfall to saturate the soil, has also increased the region's susceptibility to landslides. The existence of landslide susceptibility, the high price of land in this highland region, and population density were the main reasons for this study. This research addresses the following questions: Which area is more susceptible? Which modeling approach provides the highest accuracy? How is landslide density distributed across conditioning factors?

The simultaneous application of machine learning to complex modeling processes and the comparison of their accuracy with the frequency-ratio method, a simple statistical model, are considered the main innovations of this research. The primary goal of the study is to create a landslide

susceptibility map using ML techniques and a simple bivariate statistical method (frequency ratio) and to select the appropriate model for this task in northern Tehran. The models used in this research included the frequency ratio, GLM, and MARS. The selection of these models was based on their acceptable accuracy in many prior studies. ML techniques usually provide acceptable accuracy, but they are complex models, and the modeling process with them is complicated. Bivariate statistical models are straightforward and, if they achieve acceptable accuracy, are very practical and have a simple working method. Since model performance is highly region-dependent, it cannot be definitively stated which model type (simple versus complex) will yield higher accuracy in a specific area. Therefore, the primary innovation of the research is a systematic comparison of these two paradigms and an evaluation of their accuracy in selecting the optimal model for northern Tehran. Also in this research, the landslide density for different classes of conditioning factors is calculated. By calculating the landslide density, the susceptibility of each specified class is determined, which is valuable for regional management and planning.

Materials & Methods

Study Area

The study area is situated in the north of Tehran at 35° 47′ 30″ and 35° 58′ N latitude and 10′28°51″ and 51° 48′ 20″ E longitude, covering an area of approximately 305 Km^2 (Figure 1). The altitude varies between 1619 and 3645 m a.m.s.l. Land use in the area includes rangeland, forest, agricultural orchards, residential areas, and water bodies. The major faults in northern Tehran include Purkan-Vardij, north of Tehran, Emamzadeh Davood, and Mosha-Fasham [21]. Complex geological structures with diverse lithological formations characterize the region. According to data from Fashan station, the mean yearly rainfall is about 700 mm. Due to its milder climate compared to Tehran City, urban expansion, including the construction of gardens and roads, has occurred in this area, leading to an increase in landslide incidents. Overall, the complex geological conditions, active faults, and steep slopes favor the occurrence of landslides in northern Tehran.

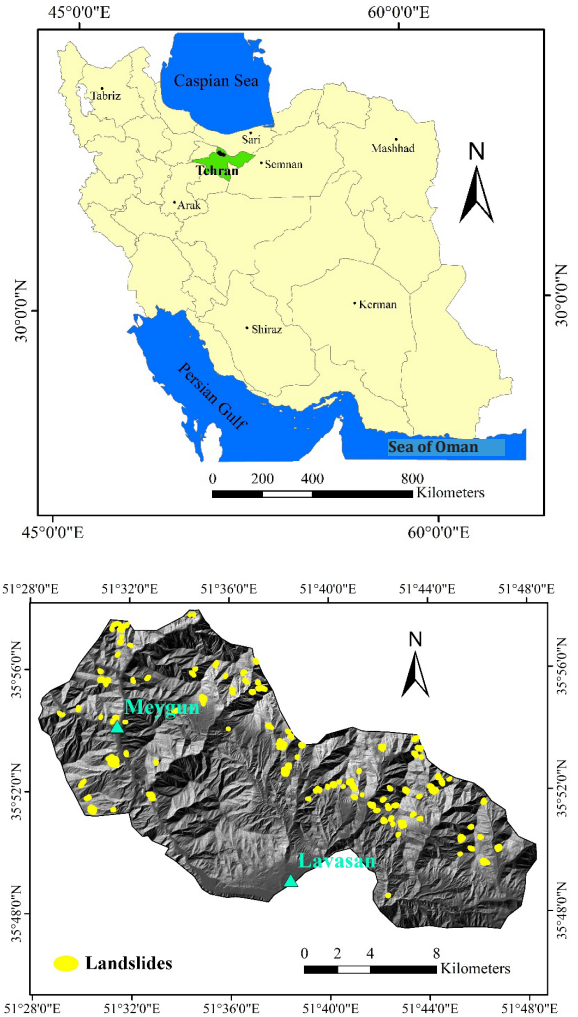

Figure 1) Location of the study area in Tehran and Iran.

Methodology

The following steps describe the research

process: (1) investigation of landslide distribution; (2) landslide susceptibility assessment using GLM, MARS, and frequency ratio models; and (3) accuracy assessment of these three models using ROC curves to identify the model most suitable for northern Tehran. Figure 2 illustrates the research methodology flowchart.

Data Preparation

Landslide Inventory Mapping

The primary inputs for creating landslide susceptibility maps are the landslide and non-landslide datasets. In this study, each point on the map was assigned a binary value: indicates the presence of a landslide, while 0 represents its absence. Historical documents, field surveys, and Google Earth of northern Tehran were used to create landslide inventory maps. To ensure comprehensive coverage, field surveys were conducted throughout the region to document both recent and historical landslide occurrences. Because the mechanisms and conditioning factors of different types of mass movements vary, only landslide events were considered in this stage. In the research area, 120 landslides were reported, covering an area of 1360–100,000 m^2. Approximately 30% of the landslides were randomly selected for validation, and the remaining 70% were utilized for modeling. The landslides cover an area of 2.45 km^2, representing about 0.8% of the total study area.

Data Collections

The conditioning factors of a landslide should

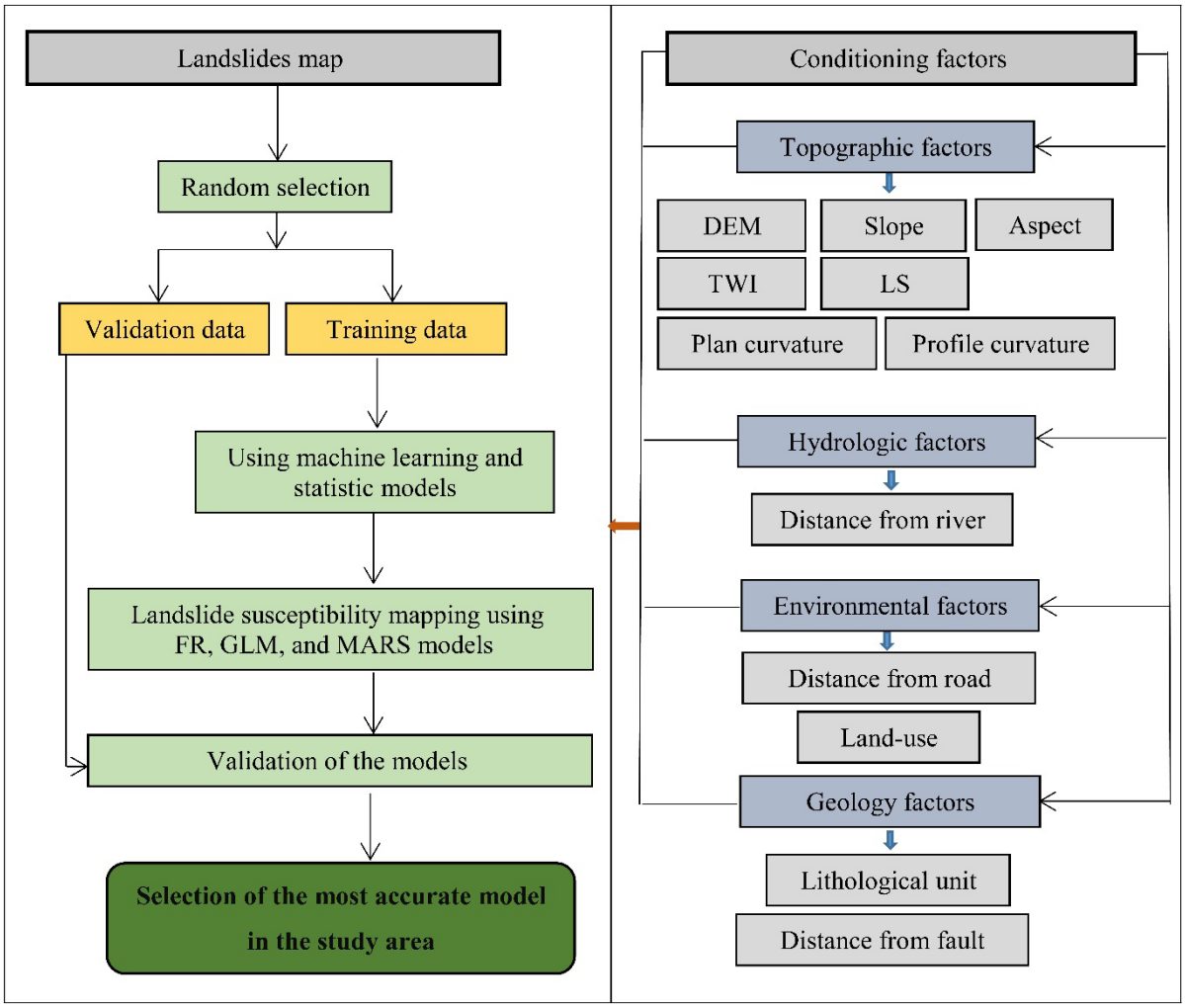

Figure 2) The flowchart of the research for the landslide susceptibility mapping.

be complete, operational, fundamental, measurable, and non-uniform [19]. There are no fixed guidelines for determining the optimal number of landslide control variables to predict landslide susceptibility, as this depends on factors such as the size and type of landslide, the landscape, and data accessibility. A review of the literature, field surveys, and considerations of data availability led to the selection of 12 factors that constituted the spatial database of landslide conditioning factors (Figure 3). Combinations of geological (lithological units and faults), morphological (slope degree, aspect, and curvature), and land-use factors are among the most commonly utilized in this field. The quality of the data mentioned above plays a vital role in machine learning models, as it affects their efficiency.

First, a 10 m resolution DEM was generated from a 1:25000-scale digitized topographic map. Elevation factors have been used in many studies as the primary factors influencing landslide occurrence. Various elevations affect other environmental factors such as temperature, rainfall, and human activity [16]. Using the DEM, slope, slope length, slope aspect, TWI, profile curvature, and plan curvature were derived. Because slope and slope instability are closely related, slope is a key factor in susceptibility mapping, influencing the dynamic characteristics of landslides and the collapse process. Aspect affects factors such as solar radiation, temperature, hydrological processes, and land cover [22]. Length of slope (LS) refers to the topographic condition of an area and can be expressed as Eq. (1) [23]

$$LS=\left[fl\times\left(\frac{\text{Pixel size}}{22.13}\right)^{0.6}\times\left(\frac{\text{Sin}(\theta)}{0.0896}\right)^{1.3}\right] \quad \text{Eq. (1)}$$

where fl denotes flow accumulation, the pixel size used was 10 m, and θ represents the slope degree.

The TWI describes the soil moisture and flow accumulation. High TWI indicates high infiltration, and these areas are more prone to landslides because water infiltration and soil saturation create conditions for them to occur. [3]. Changes in ground slope are indicated by profile curvature, which can be used to predict landslides. The contour curvature is described by plane curvature, which affects runoff volume [24].

The drainage network was extracted using a topographic map. The buffer tool in ArcGIS (https://www.esri.com) was used to determine the distance from the streams. Generally, landslide susceptibility decreases with increasing distance from drainage channels [20]. Highly fractured rocks near faults are less stable under seismic activity, and proximity to faults significantly increases landslide risk. Distances from the faults and road maps were calculated using GIS. A land-use map was produced from LANDSAT 8 images (2023) using an integrated ENVI technique. In general, land-use and land-cover characteristics influence the resistance of slopes to landslides. Plant roots can protect steep slopes and are usually considered soil protectors [19]. A lithological map (scale 1:100000) was prepared in the GIS environment using a geology map from the Geological Survey of Iran. The lithological conditions in northern Tehran were grouped into seven main categories (Table 1). Lithology is a key factor in landslide susceptibility assessments [25]. It is generally accepted that lithological features significantly affect the permeability and strength of the material, thereby influencing landslides [19]. The general characteristics of

all base maps are summarized in Table 2. The correlation among the conditioning factors was assessed using a multicollinearity test in SPSS. A VIF value below five and a tolerance value above 0.1 indicate an acceptable level of independence among variables [26]. The computed multicollinearity statistics are presented in Table 3. There was no correlation between factors in this research.

Landslide Susceptibility Mapping

Frequency Ratio (FR)

The correlation between landslide occurrences and conditioning factors can

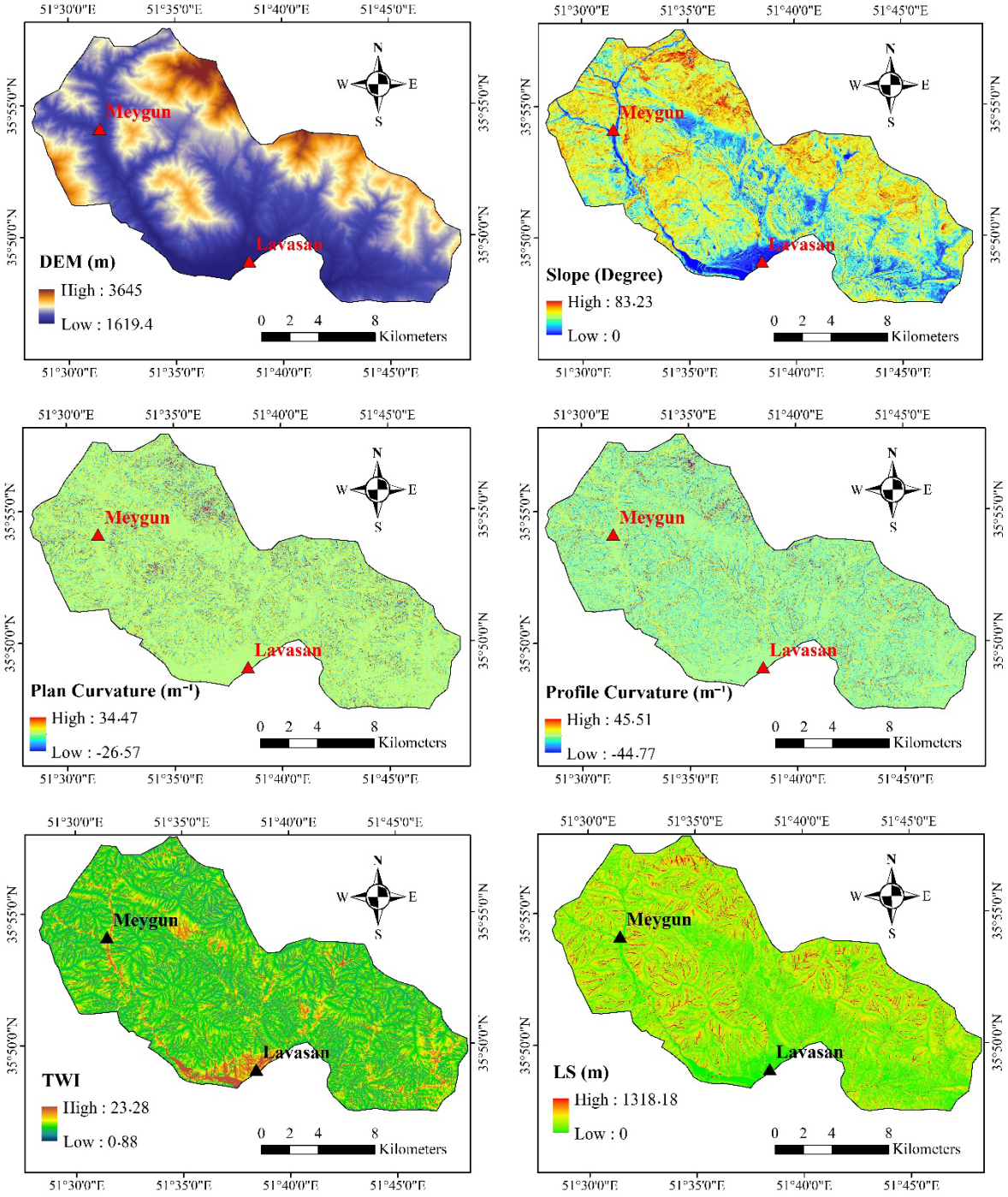

Figure 3) Maps of conditioning factors in the north of Tehran.

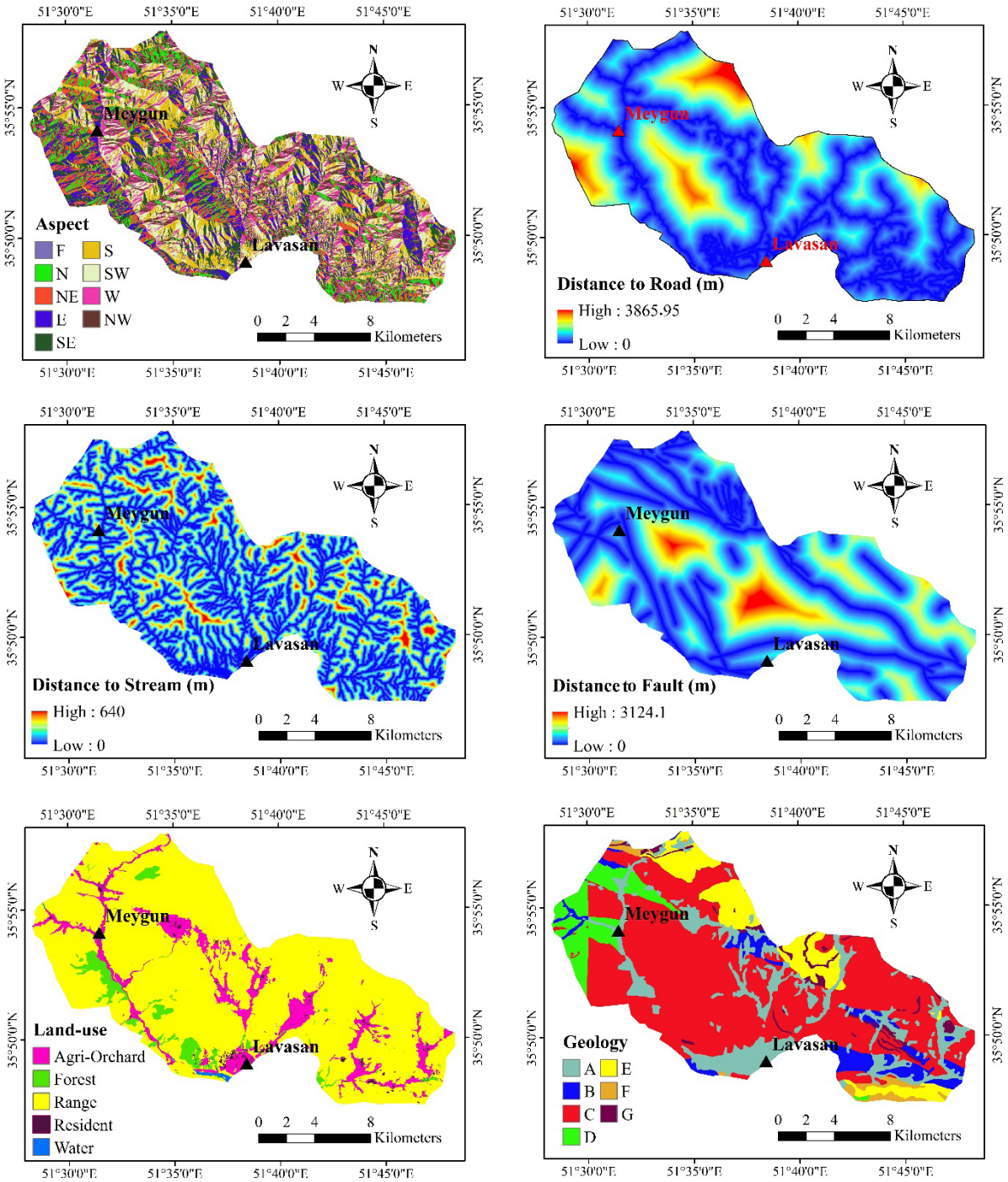

Figure 3 Continued) Maps of conditioning factors in the north of Tehran.

be inferred by comparing the proportions of landslide areas within each factor class. The discrepancy in each score between the landslides and conditioning factors in each class can be easily explained by the frequency ratio [19]. The FR value shows the strength of association between landslides and a particular class of conditioning factors. The frequency ratio was determined using Eq. (2) [16] in the ArcGIS environment:

$$FR = \frac{Ni}{N0} / \frac{Si}{S0} \qquad \text{Eq. (2)}$$

where Ni indicates the number of landslides

Table 1) Lithology of northern Tehran.

Group	Lithology	Group	Lithology
A	Young Alluvia Fans	D	Tuffaceous
	Old Alluvial Fans		Shales and Siltstone
	Talus Deposits		Green Tuffs
	Young and Old Terraces, Residual Soils		Gypsum
	Conglomeratic Terraces	E	Marl, Sandstone, Gypsum
	Morain		Thick-Bedded Polygenetic Conglomerate
	Scree		Andesitic–Dacitic Rocks, Pyroclastic, Tuffs
	Young Terraces		Thin-Bedded Limestone
	Old terraces		Thin-Bedded To Massive Limestone
	Sandstone		Marly limestone, marl
	Miocene Deposits (Conglomerate, Sandy Marl, Miliolidus limestone)		Sandstone, Siltstone, Clay Stone
B	Sandstone, Mudstone, Siltstone	F	Dolomitic Limestone
	Conglomerate, Gypsum		Massive Limestone
	Conglomerate, Tuff		Platy Limestone,
	Sandstone, Green Tuff		Marly Limestone
	Tuffaceous Sandstone		Medium-Bedded Limestone
	Tuffite Sandstone		Gray Limestone
	Red Conglomerate		Gray Massive Dolomitic Limestone
C	Medium-Thin-Bedded Limestone		Black Limestone, Clayey Marl Intercalations
	Green Micaceous Shales		Intraclastic Limestone
	Conglomerate, Gypsum		Dolomitic Limestone
	Gray Laminated Mudstone		Sandstone, Shale
	Calcareous and Siliceous Shale		Trilobite-Bearing Limestone, Marl
	Shale and Tuffaceous Sandstone		White Quartzite, Quartzitic Sandstone
D	Tuff Breccia	G	Red Arkosic Sandstone
	White and Green Tuff Breccia		Siltstone and Shale
	Rhyolitic Tuff		Black Massive Dolomite
	Massive Green Tuff		Basic and Intermediate Sills
	conglomerate, and Limestone		Leuosyenite Porphyry
	Rhyolitic Tuff		Dacitic Dikes
	Bituminous Siltstone and Shale		Brown Shale and Siltstone

Table 2) Specifications of Base Maps.

Map	Data source	Format	Resolution	Preprocessing
Topographic Map	National Cartography Center of Iran	Vector	1:25000	-
Drainage Network	National Cartography Center of Iran	Vector	1:25000	Distance Calculation
Roads	National Cartography Center of Iran	Vector	1:25000	Distance Calculation
Faults	Iranian Geological Survey	Vector	1:100000	Distance Calculation
Lithological Map	Iranian Geological Survey	Vector	1:100000	Convert to Raster
LANDSAT 8 Images	USGS	Raster	-	Classification

Table 3) Determine the Correlation between the study factors affecting landslide susceptibility assessment of Tehran Province.

Model	Std. Error	Beta	t-Value	Sig. Level	Tolerance	VIF
Constant	0.079	-	-19.735	0.000	-	-
Plan Curvature	0.005	-0.005	-0.392	0.695	0.640	1.563
LS	0.000	-0.042	-2.729	0.006	0.402	2.486
Lithology	0.046	-0.008	-0.755	0.450	0.926	1.080
Land-Use	0.011	0.149	13.657	0.000	0.808	1.238
Distance to Fault	0.000	-0.061	-5.892	0.000	0.905	1.105
Elevation	0.000	0.395	26.646	0.000	0.438	2.282
TWI	0.005	0.170	9.599	0.000	0.307	3.260
Distance to Drainage	0.000	0.070	6.396	0.000	0.803	1.246
Slope	0.001	0.228	14.492	0.000	0.387	2.587
Aspect	0.017	0.109	10.486	0.000	0.886	1.128
Distance to Road	0.000	-0.263	-18.475	0.000	0.475	2.104
Profile Curvature	0.005	-0.020	-1.912	0.056	0.838	1.193

in class i of a conditioning factor. N0 displays the total number of landslides, Si is the area of class i of this factor, and S0 is the total area of the region. A FR value greater than 1 indicates that the landslide density in that class is higher than the average density of the region. FR values below 1 indicate a lower density of landslides within that class [16]. The calculated FR weights were incorporated into the ArcGIS environment to create a susceptibility map.

Generalized Linear Model (GLM)

The GLM is a statistical approach used to describe the relationship between the dependent and the independent variables. Additionally, it resembles a multiple regression approach [27]. The GLM model is introduced for maximum-likelihood modeling. Regression provides the basis for defining the GLM algorithm and can demonstrate how the components differ [28]. The GLM was fitted with a binomial family and a logit link, which is appropriate for binary (landslide/non-landslide) data and allows straightforward interpretation in terms of odds ratios. GLM displays a linear predictor as Eq. (3) [29]:

$$E(Y)=\mu \times g^{-1}(X\beta) \quad \text{Eq. (3)}$$

where E(Y), Xβ, and g are the expected values of Y, the linear predictor, and the link function, respectively.

The variance is a function of μ:

$$Var(Y)=V_{(\mu)}=V(g^{-1}(X\beta)) \quad \text{Eq. (4)}$$

where Bayesian models can be used to estimate the β parameter.

Multivariate Adaptive Regression Spline (MARS)

The MARS approach is a nonparametric, data-driven method for modeling complex, nonlinear relationships between dependent and independent variables [30]. Eq. (5) defines this as a weighted basic function:

$$F(x)=a_0+\sum_{i=1}^{n} a_i f_i(x) \quad \text{Eq. (5)}$$

where $f_i(x)$, n, and $f_0(x)$ are the basic functions, basic function number, and coefficient of a_0. Ordinary least squares (OLS) is employed to compute every coefficient, whereas the basic functions are calculated using Eq. (6).

$$f_i(x)=\prod_{fl}^{d_i}\left[S_{fi}(X_{v(f,i)}-t_{fi})\right] \quad \text{Eq. (6)}$$

where d_i is the variable number in the ith basic function S_{ji}, $Xv(_{j,i})$ is the vth variable, $1 \le v(j,i) \le d$, and t_{ji} is the knot location of the corresponding variable [31]. Specifically, the MARS model was developed with 12 independent variables and, after pruning, retained 14 basic functions, selected using the minimum generalized cross-validation (GCV5) criterion.

Both machine learning models (GLM and MARS) were implemented in R, and the resulting coefficients were imported into ArcGIS to produce landslide susceptibility maps.

Accuracy Assessment

Model performance was evaluated to identify the most suitable method for landslide susceptibility mapping in northern Tehran. The ROC and the area under the curve were used to assess model quality. Approximately 70% of the mapped landslides were used to map susceptibility during the modeling process. 30% of the landslides were reserved for model verification. Eq. (7) was used to determine the ROC curve.

$$AUC=\frac{\sum TP+\sum TN}{PN} \quad \text{Eq. (7)}$$

where P and N are landslide and non-landslide points. The true positive and true negative classes are denoted as TP and TN, respectively [20]. In addition, sensitivity, specificity, Cohen's kappa index, and fourfold cross-validation were utilized to validate the models [32]. The Landslide Density Index (LDI) was also used to evaluate the accuracy of the prepared maps. The density of landslides within each susceptibility class is used to determine the LDI. Higher landslide densities in high-susceptibility zones indicate greater model accuracy [33].

Findings

Frequency Ratio Model

To create a map of susceptibility using the FR model, total conditioning factor maps were classified, and the weight of each class was then calculated using equation 2 (Table 4). Finally, the FR values were entered into the GIS, and landslide susceptibility was mapped.

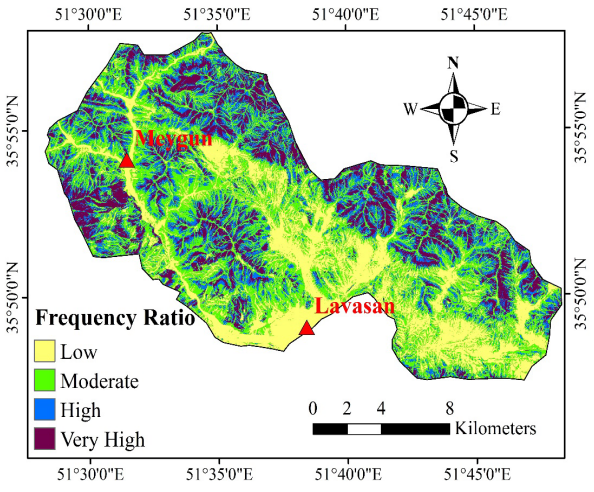

Figure 4) Map of landslide susceptibility made with the FR model.

Table 4) Frequency ratio of each conditioning factor class.

Factor	Attributes	Ni	Si	FR
Elevation/DEM (meter)	<1970	260	602502	0.305
	1970-2240	1018	924465	0.780
	2240-2500	1260	709088	1.259
	2500-2900	1291	588169	1.555
	>2900	474	225196	1.492
Slope (degree)	<8	7	189502	0.026
	8_17	99	363668	0.193
	17-25	655	583483	0.796
	25-40	3158	1668809	1.341
	>40	384	243958	1.115
Aspect	F	7	6223	0.797
	N	258	260458	0.702
	NE	675	299325	1.598
	E	690	353907	1.382
	SE	665	423269	1.113
	S	605	502041	0.854
	SW	476	516904	0.653
	W	579	382869	1.072
	NW	344	304424	0.801
Plan Curvature (m^{-1})	<-0.01	2121	1380146	1.089
	-0.01-0.01	212	146865	1.023
	>0.01	1970	1522409	0.917
Profile Curvature (m^{-1})	<-1	611	461350	0.939
	-1-1	3007	2103494	1.013
	>1	685	484576	1.012
LS (meter)	<18	655	1184200	0.392
	18-35	2432	1281467	1.345
	35-130	1208	557881	1.535
	>130	8	25872	0.219
TWI	<4.5	792	885979	0.634
	4.5-6	2291	1325557	1.225
	6-11.5	1217	767749	1.123
	>11.5	3	70135	0.030
Distance to Road (m)	<400	1647	1302590	0.896
	400-900	1326	778475	1.207
	900-1500	751	511394	1.041
	1500-2200	298	306047	0.690
	>2200	281	150914	1.120

GLM and MARS Model

After implementing the GLM and MARS in R, the resulting susceptibility values were imported into GIS to produce a susceptibility map. Using the natural break technique [11], maps were divided into low, moderate, high, and very high susceptibility categories (Figures 5 and 6).

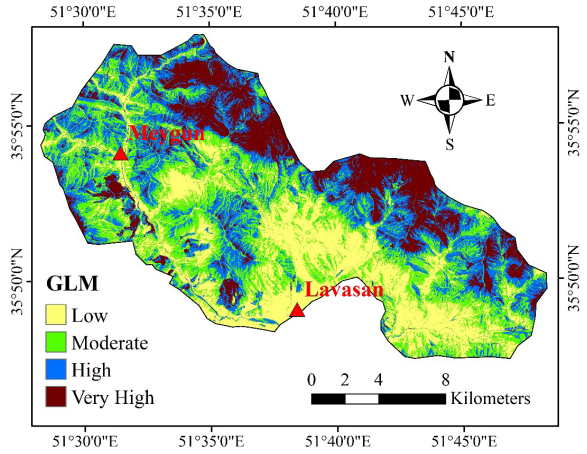

Figure 5) Map of landslide susceptibility made with the GLM model.

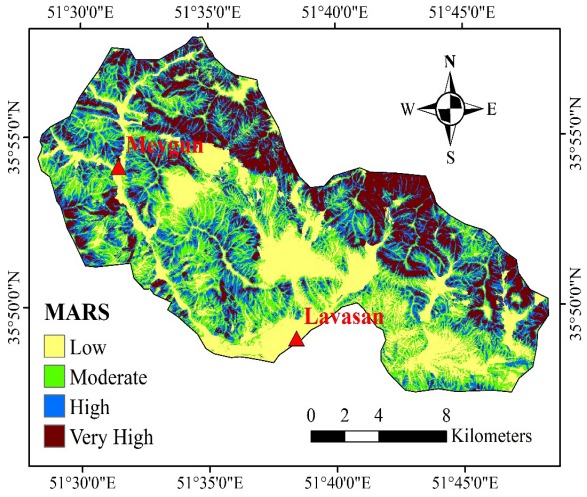

Figure 6) Map of landslide susceptibility made with the MARS model.

Accuracy Assessment of the Models

The area under the ROC curve (AUC) for FR, GLM, and MARS was 0.755, 0.751, and 0.808, respectively (Figure 7 and Table 5). The relationship between the models' accuracy and AUC was expressed as follows: weak (0.5–0.6), moderate (0.6–0.7), well (0.7–0.8), very well (0.8–0.9), and excellent (0.9–1) [34].

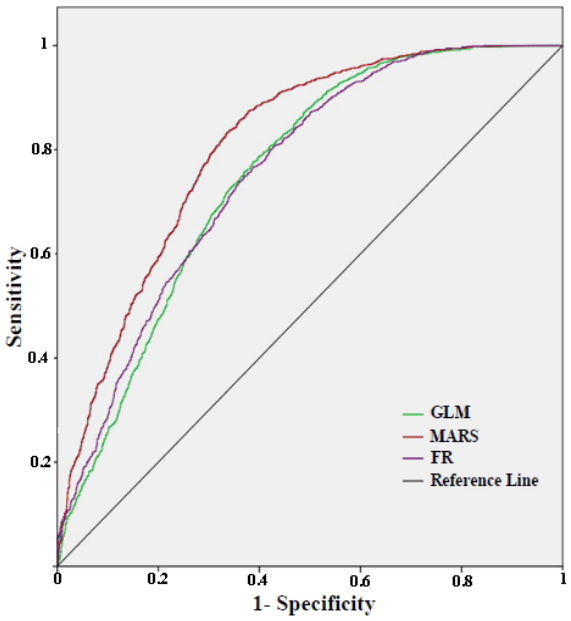

Figure 7) ROC curve of the models used in the study area.

Table 5) Statistical indices for the applied models.

Model	Area	Standard Error	Asymptotic 95 % Confidence Interval	
			Lower Bound	Upper Bound
GLM	0.751	0.008	0.735	0.767
MARS	0.808	0.007	0.794	0.822
FR	0.755	0.008	0.710	0.771

The results of the sensitivity, specificity, fourfold cross-validation, and Cohen's kappa index are presented in Figures 8 and 9.

The findings demonstrated that the MARS model's accuracy was very good (0.808). The MARS model exhibited the highest accuracy. The LDI values for the GLM, MARS, and FR models were 1.58, 2.93, and 1.63, respectively. The LDI results were also consistent with the ROC curve results, identifying the MARS model as the most accurate. The accuracies of the FR and GLM models were good (0.755 and 0.751, respectively) in northern Tehran.

Table 4 Continued) Frequency ratio of each conditioning factor class.

Distance to Stream (m)	<70	698	954692	0.518
	70-160	1363	998164	0.968
	160-250	1157	597970	1.371
	250-370	996	407788	1.731
	>370	89	90806	0.695
Distance to Fault (meter)	<450	2116	1340322	1.119
	450-1000	1156	886078	0.925
	1000-1700	929	608864	1.081
	>1700	102	214156	0.338
Geology/Lithological Units	A	749	516807	1.027
	B	243	170290	1.011
	C	2286	1728364	0.937
	D	282	201520	0.992
	E	490	307915	1.128
	F	111	53752	1.463
	G	138	70765	1.382
Land-Use	Agriculture-Garden	195	339423	0.407
	Forest	472	117512	2.846
	Rangeland	3617	2555951	1.003
	Residential	15	29108	0.365
	Waterbody	0.01	7426	0.001

Areas of the Susceptibility Classes

The region's landslide susceptibility can be demonstrated by comparing the areas of the susceptibility classes. A large portion of the area in high-susceptibility classes indicates the region's overall susceptibility. The areas of the susceptibility classes were calculated using susceptibility maps (Table 6). The results show that approximately 37% (FR) to 44% (MARS) of the study area has high to very high susceptibility in the models.

Table 6) Area of total susceptibility classes for applied model.

Model	Susceptibility Classes Area (km^2)			
	Low	Moderate	High	Very High
FR	77.982	112.742	64.014	50.203
GLM	81.476	88.487	81.504	53.475
MARS	86.995	81.768	75.998	60.181

Discussion

Based on the weight derived from the FR model (Table 4), the elevation class of 2,500-2,900 was identified as the most susceptible. Lower elevations in the study area generally have lower slopes, and areas with very high elevations (>2900 m) are almost uninhabited. Therefore, the effect of human endeavors, such as road construction, on the instability of geological bodies is limited. Similarly, Mosaffaie et al. [35] reported that intermediate elevation zones in the Alamut watershed exhibited higher landslide susceptibility. Elevation is one of the most significant landslide-driving factors and can intentionally alter the quantity, number, intensity, and extent of landslides. Elevation indirectly controls several landslide-related variables, including temperature, precipitation, frost

effects, and ice melting. Consistent with these findings, Pourghasemi et al. [36] identified elevation and land use as the two most important factors affecting landslides in Iran. Hong [37] showed that elevation was the most significant conditioning factor for landslides in Yongxin County, China. The analysis of landslide density by slope class showed that the 25-40° slope class had the highest FR values. Slope maps are commonly used in landslide research because landslides are directly related to slope steepness. Slope steepness can significantly reduce soil cohesiveness and increase the shear stress. When slopes exceed 25°, the likelihood of a landslide may increase [38]. Gentle slopes are expected to experience fewer landslides because of the low shear stresses [19]. On very steep slopes (greater than 40°), the frequency of landslides decreased again because the slope has remained steep today, mainly due to the lack of potential for landslides. The shallow soil depth and the lack of sufficient soil for landslides to occur may also explain the decrease in landslides in these areas. Previous studies have also shown the importance of slope [9, 16, 19]. The slope aspect analysis revealed that the northeastern and eastern slopes had the highest FR values. The northeastern and east slopes usually receive less moisture, resulting in weaker vegetation and greater susceptibility to landslides. The aspect is a key factor that governs the occurrence of landslides through its effects on solar radiation, moisture, seepage direction, rainfall, and other critical factors [24]. Other researchers, including Dai et al. [25] and Yuvaraj and Dolui [19], have emphasized the significance of the slope aspect. Among other topographic parameters, plan curvature less than -0.01, profile curvature -1 to 1, slope length of 35-130, and TWI of 4.5-6 demonstrated the highest sensitivity to landslides. These factors affect water retention and runoff, thereby influencing landslides. Asmare [13], Guo et al. [16], Chowdhury et al. [3], and Rai et al. [9] also pointed out the importance of these factors in their studies. For the distance from the stream, the frequency ratio was highest in the 160-370 meter class. Streams and rivers can alter the groundwater distribution and erode hillsides. Therefore, a significant factor influencing this is the distance between them [9, 14, 16, 20]. Generally, it is expected that the distance less than the stream will have higher susceptibility. However, it was observed that the susceptibility of classes less than 160 is not higher than that of classes from 160 to 370. The reason is bank erosion of the stream, which prevents soil accumulation and landslide formation. Also, within a very short distance of streams, there is usually good vegetation cover, which helps prevent landslides. A distance of 400-900 m from the road showed the highest landslide susceptibility. The road alters the region's physiographic conditions and imposes greater weight on the region due to vehicle traffic. Road construction across hilly, steep terrain weakens the rock mass and increases the risk of landslides [39]. Roads also significantly affect hydrological response, leading to changes in runoff and soil degradation [28]. Very close to roads, protective structures, and stabilization measures may reduce landslide occurrence, while areas slightly farther away (400–900 m) experience greater instability. As shown in Table 4, areas within 450 m of faults are highly susceptible to landslides. Roback et al. [40] explained that landslides largely depend on the number and density of the active faults. Li et al. [14] and Ahmad et al. [18] introduced faults as major

contributors to landslide occurrence.

Investigating the frequency of landslides in geological formations showed that Group F formations (limestone, marly limestone, marl, sandstone, shale, clay stone, siltstone, dolomites, black limestone, clayey marl intercalations, and trilobite-bearing limestone) were the most susceptible to landslides. These salt-bearing, fine-grained materials readily absorb water, leading to a loss of strength and slope failure. Therefore, these formations in northern Tehran are more susceptible to landslides. Lithology is a crucial factor as it affects the physical properties of soils and rocks, such as their permeability and strength. Hence, many researchers have used this factor in their studies and have emphasized its role in landslide occurrence [9, 37]. Among the land-use categories in northern Tehran, forests showed the highest susceptibility. Forests are usually located on steep slopes where other landslide conditions are present, which is why they are among the most susceptible to landslides. In bivariate models, because it is not possible to consider the simultaneous effects of all factors, the weight assigned to a category can be unexpected, reflecting the dominance of other factors in that category. For example, it is generally expected that

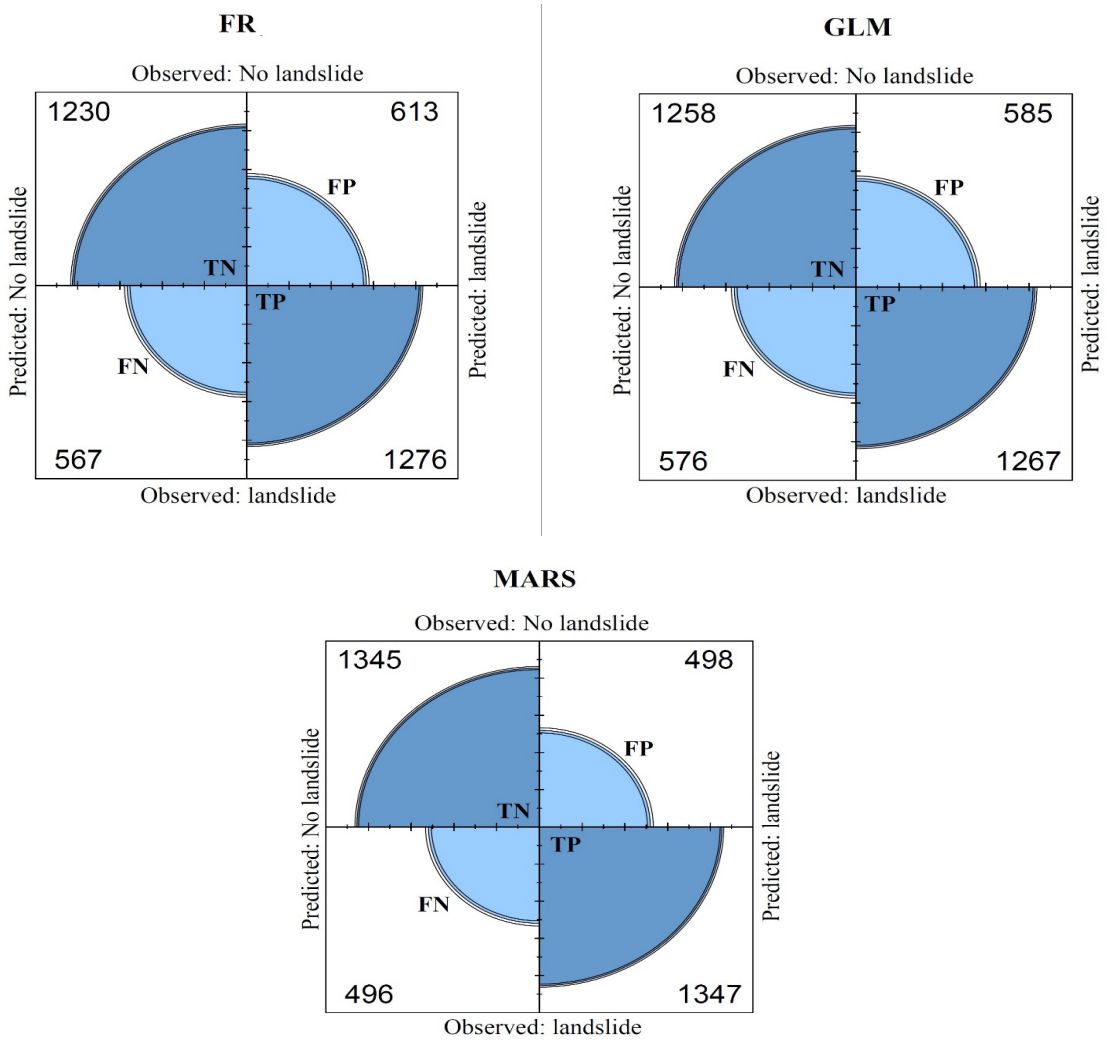

Figure 8) Fourfold plots of FR, GLM, and MARS models.

landslides will be less frequent in forests, but because other factors dominate, this land use class has shown high susceptibility. The validation of the models showed that the MARS model has the highest accuracy in the study area. The MARS model's superior performance can be attributed to its versatility, precision, and efficiency in modeling both continuous and binary outcomes. The primary advantages of the MARS model are its additive and interactive structure, and reduced number of variable interactions. In addition, the MARS model can be applied in a forward and backward stepwise procedure [41]. Other researchers, including Zheng et al. [42], Mohammady [43], and Rai et al. [9], also confirmed the model's accuracy in their studies. In general, machine

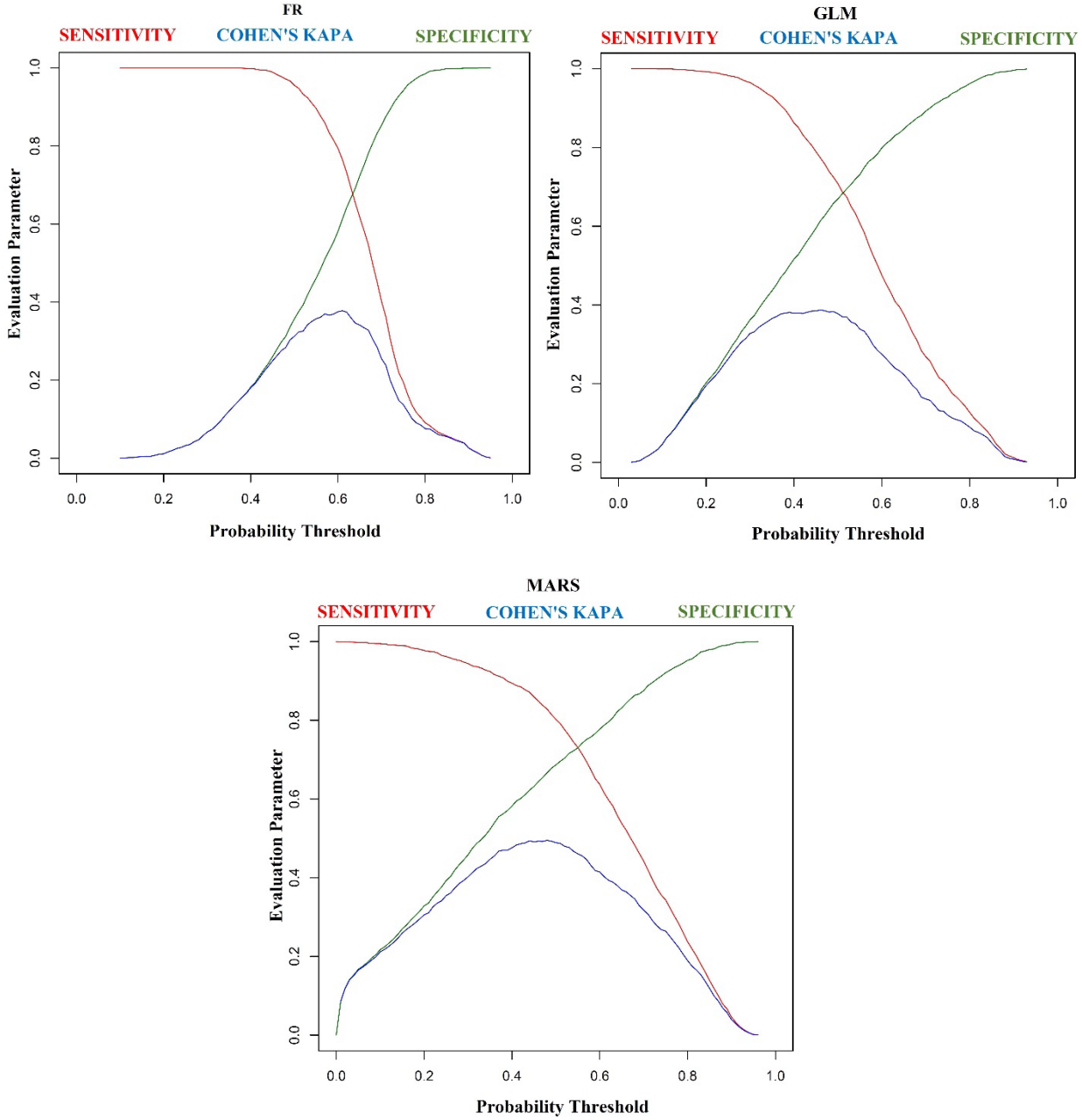

Figure 9) Fitting performance measures of FR, GLM, and MARS models.

learning techniques have acceptable accuracy in susceptibility mapping and have been used in many geo-environmental studies. Numerous datasets can be handled, generalized, and accurately represented by machine-learning algorithms [44]. Despite their advantages, machine-learning techniques require a solid understanding of predictive variables because they have demonstrated relationships between landslide conditioning variables and landslides. Therefore, these models can be used by any researcher with expertise in statistics and machine learning [9]. These models, like many other models, also have limitations. The major drawback of machine learning is its reliance on training data [9].

The frequency-ratio approach, widely used in landslide research, can capture the nonlinear relationship between the basic environment and landslide susceptibility. The most significant benefit of the frequency ratio model is its ease of use. Therefore, various researchers have used this model and confirmed its accuracy despite its simplicity [10, 12, 16, 17, 19]. For example, Mosaffaie et al. [45] used the Statistical index, frequency ratio, and AHP to assess the landslide susceptibility in the Shahroud watershed, Qazvin. The results indicated that the accuracy of the two statistical models exceeded that of the AHP model.

One of the most common natural phenomena in mountainous regions is landslides, which abruptly alter local terrain and cause significant damage to agricultural lands, roads, residential areas, and other infrastructure. Hence, reducing landslide losses is an essential research topic [34]. Susceptibility analysis of these areas is crucial for building highway corridors, developing infrastructure, and preventing and reducing landslide-related disasters. The calculated area indicates that the region is highly susceptible to landslides, underscoring the need for careful attention to this natural hazard. Geographical datasets and landslide susceptibility maps will be helpful for sustainable hill planning in the area, land-use planning, and identification of vulnerable regions. The use of the susceptibility map in land use planning and multi-hazard assessment has been proposed in other studies, including Salehpour Jam et al. [46] and Salehpour Jam et al. [47] in the Alamut watershed and the Razmian region, respectively. Similarly, his study contributes to this growing body of knowledge by offering insights that help stakeholders, policymakers, and the scientific community make informed decisions. We can utilize low-susceptibility zones for upcoming development projects by identifying them, whereas mapping high- and very-high-susceptibility zones requires reducing the risk to infrastructure and life. Landslides cause damage to residential areas and infrastructure, including roads, every year. The best solution to prevent damage is to identify susceptible areas and control development in these areas. A landslide susceptibility map can serve as a fundamental tool for land-use planning, risk analysis for infrastructure development, and other policies in this region. Paying attention to the landslide susceptibility map will play a significant role in preventing capital waste and preserving natural resources and the environment. It is recommended that, in multi-hazard assessments, landslides be considered an important hazard in northern Tehran, alongside other hazards.

Conclusion

Due to its geological and topographic conditions, the north of Tehran is continually exposed to landslides. Hence, a precise and accurate map of landslide susceptibility is

essential for natural resource managers, policymakers, and land-use planners to develop and apply applicable mitigation measures. A landslide susceptibility map for northern Tehran was prepared using two machine learning models (GLM and MARS) and a bivariate statistical model (Frequency ratio). The findings indicated that the FR and GLM models demonstrated good accuracy, while the MARS model showed very good accuracy in the study area. The areas of the susceptibility classes were calculated, and approximately 37% (FR) to 44% (MARS) of the region has high or very high susceptibility in the models. These findings indicate that the region is highly prone to landslides, warranting immediate attention and careful management. Effective watershed management depends on the identification, categorization, and zonation of landslide-prone areas, which are critical elements in assessing environmental threats. Geographical datasets and landslide susceptibility maps will be helpful for sustainable hill planning in the area, land-use planning, and identification of vulnerable regions. The evaluation of the models' accuracy indicates their suitability for northern Tehran, but this research has certain limitations that can be addressed in future research. The use of soil data such as depth, texture, and chemical composition is recommended for future research. Another limitation is the absence of rainfall data as a conditioning factor. Due to the limited number of rainfall stations and the challenges of spatial interpolation, it is recommended that rainfall be derived from satellite data for future studies. Additionally, future work should explore other modeling approaches, including multivariate models and expert opinion-based models, to identify the most suitable model for the region with greater confidence. Continuous monitoring of new landslides is also recommended to enhance validation of susceptibility maps, as comparing newly occurring landslides with predicted highly susceptible zones would provide stronger evidence of model reliability.

Acknowledgments

This research was funded by Semnan University (research grant No. 14026). The author wish to thank Semnan University for making this research possible.

Author's Contribution: All stages of the research have been carried out by Majid Mohammady.

Ethical Permission: None declared

Conflict of Interest: The author declares that they have no conflicts of interest.

References

1. Fang Z., Wang Y., Peng L., Hong H. Integration of convolutional neural network and conventional machine learning classifiers for landslide susceptibility mapping. Comput. Geosci. 2020; 139: 104470.
2. Froude M., Petley D. Global fatal landslide occurrence from 2004 to 2016. Nat. Hazard. Earth Syst. Sci. 2018; 18(8): 2161–2181.
3. Chowdhury S., Rahman N., Sheikh S., Sayeid A., Mahmud K.H., Hafsa B. GIS-based landslide susceptibility mapping using logistic regression, random forest, and decision and regression tree models in Chattogram District, Bangladesh. Heliyon. 2024; 10: e23424.
4. Iranian Landslide Working Party (ILWP) (2007). Iranian landslides list, Forest, Rangeland and Watershed Association, Iran.
5. Shoaei Z., Ghayoumian J. Toward the Mechanism of Deadly Landslide and Debris Avalanche in Abikar Village, Farsan City, Chaharmahal and Bakhtiari Province, Iran. ECOPERSIA 2022; 10(4):297-309.
6. Hadian Amri M., Solaimani K., Kavian A., Afzal P. A new approach to landslide assessment using the Depth-Number fractal model. ECOPERSIA 2023; 11(1):11-23.
7. Liu X.D., Xiao T., Zhang S.H., Sun P.H., Liu L.L., Peng

Z.W. Comparative study of sampling strategies for machine learning-based landslide susceptibility assessment. Stoch. Environ. Res. Risk Assess. 2024; 38(12): 4935–4957.
8. Youssef K., Shao K., Moon S., Bouchard L.S. Landslide susceptibility modeling by interpretable neural network. Commun. Earth Environ. 2023; 4(1):162.
9. Rai S.C., Pandey V.K., Sharma K.K., Sharma S. Landslide susceptibility analysis in the Bhilangana Basin (India) using GIS-based machine learning methods. Geosyst. Geoenviron. 2024; 3(2): 100253.
10. Khan H., Shafique M., Khan M.A., Bacha M.A., Shah S.U., Calligaris C. Landslide susceptibility assessment using Frequency Ratio, a case study of northern Pakistan. Egypt J Rem Sens Space Sci. 2019; 22(1): 11–24.
11. Mohammady M., Pourghasemi H.R., Pradhan B. Landslide susceptibility mapping at Golestan Province, Iran: a comparison between frequency ratio, Dempster-Shafer, and weights of evidence models. J. Asian Earth Sci. 2012; 61 (1):221–236.
12. Alsabhan A.H., Singh K., Sharma A., Alam S., Pandey D.D., Rahman S.A.S., Khursheed A., Munshi. F.M. Landslide susceptibility assessment in the Himalayan range based along Kasauli–Parwanoo road corridor using weight of evidence, information value, and frequency ratio. J. King Saud Univ. Sci. 2022; 34(2): 101759.
13. Asmare D., Application and validation of AHP and FR methods for landslide susceptibility mapping around Choke Mountain, northwestern Ethiopia. Sci. Afr. 2023; 19: e01470.
14. Li M., Wang H., Chen J., Zheng K. Assessing landslide susceptibility based on the random forest model and multi-source heterogeneous data. Ecol. Indic. 2024;158:111600.
15. Zhang W., Liu S., Wang L., Samui P., Chwała M., He Y. Landslide susceptibility research combining qualitative analysis and quantitative evaluation: A case study of Yunyang County in Chongqing, China. Forest. 2022; 13(7):1055.
16. Guo Z., Guo F., Zhang U., He J., Li G., Yang Y., Zhang X. A Python system for regional landslide susceptibility assessment by integrating machine learning models and its application. Heliyon. 2023; 9(11): e21542.
17. Zhang A., Zhao X.W., Zhao X.Y., Zheng X.Z., Zeng M., Huang X., Wu P., Jiang T., Wang S.C., He J., Li Y.Y. Comparative study of different machine learning models in landslide susceptibility assessment: A case study of Conghua District, Guangzhou, China. China Geol. 2024; 7(1):104–115.
18. Ahmad M.S., Lisa M., Khan S. Comparative analysis of analytical hierarchy process (AHP) and frequency ratio (FR) models for landslide susceptibility mapping in Reshun, NW Pakistan. Kuwait J. Sci. 2023; 50(3): 387–398.
19. Yuvaraj R.M., Dolui B. Geographical assessment of landslide susceptibility using a statistical approach. Quat. Sci. Adv. 2023; 11:100097.
20. Bisht S., Rawat K.S., Singh S.K. Earth observation data and GIS-based landslide susceptibility analysis through frequency ratio model in the Lesser Himalayan region, India. Quat. Sci. Adv. 2024;13:100141.
21. Geology Survey of Iran (GSI). 1997.
22. Sevgen E., Kocaman S., Nefeslioglu H.A., Gokceoglu C.A. Novel performance assessment approach using photogrammetric techniques for landslide susceptibility mapping with logistic regression, ANN, and random forest. Sensor. 2019; 19(18):3940.
23. Zakerinejad R., Maerker M. An integrated assessment of soil erosion dynamics with special emphasis on gully erosion in the Mazayjan basin, southwestern Iran. Nat. Hazard. 2015; 79(S1):25–50.
24. Zeng T., Wu L., Peduto D., Glade T., Hayakawa Y.S., Yin K. Ensemble learning framework for landslide susceptibility mapping: Different basic classifier and ensemble strategy. Geosci. Front. 2023; 14(6):101645.
25. Dai F.C., Lee C.F., Li J.X.Z.W., Xu Z.W. Assessment of landslide susceptibility on the natural terrain of Lantau Island, Hong Kong. Environ. Geol. 2001; 40(3):381–391.
26. O'Brien R.M. A caution regarding rules of thumb for variance inflation factors. Qual Quant. 2007; 41(5): 673-690.
27. Atkinson P., Jiskoot H., Massari R., Murray T. Generalized linear modelling in geomorphology. Earth Surf. Process Landf. 1998; 23(13): 1185-1195.
28. Mohammady M., Davudirad A. Gully Erosion Susceptibility Assessment Using Different Machine Learning Algorithms: A Case Study of Shazand Watershed in Iran. Environ. Model. Assess. 2024; 29(2): 249–261.
29. Nordin N.D., Zan M.S.D., Abdullah F. Generalized linear model for enhancing the temperature measurement performance in Brillouin optical time domain analysis fiber sensor. Opt. Fiber Technol. 2020; 58:102298.
30. Felicísimo Á.M., Cuartero A., Remondo J., Quirós E. Mapping landslide sus-ceptibility with logistic regression, multiple adaptive regression splines, classi-fication and regression trees, and maximum entropy methods: a comparative study. Landslides. 2013; 10(2): 175–189.
31. Chu L., Wang L.J., Jiang J., Liu X., Sawada K., Zhang J. Comparison of landslide susceptibility maps using random forest and multivariate adaptive regression spline models in combination with catchment map

units. Geosci. J. 2019; 23(2): 341–355.
32. Mohammady M., Pourghasemi H.R., Amiri M., Tiefenbacher J.P. Spatial modeling of susceptibility to subsidence using machine learning techniques. Stoch. Environ. Res. Risk. Assess. 2021; 35(8):1689–1700.
33. Dhakal D., Singh K. A Geospatial Approach to Landslide Susceptibility Mapping of Spiti, India. J. Min. Environ. 2025; 16(1): 183-205.
34. Yesilnacar E.K. The application of computational intelligence to landslide susceptibility mapping in Turkey. PhD Thesis, Department of Geomatics, the University of Melbourne. 2005; p: 423.
35. Mosaffaie J., Salehpour Jam A., Sarfaraz F. Landslide risk assessment based on susceptibility and vulnerability. Environ. Dev. Sustain. 2024a; 26(4): 9285–9303.
36. Pourghasemi H.R., Mohammady M., Pradhan B. Landslide susceptibility mapping using index of entropy and conditional probability models in GIS: Safarood Basin, Iran. Catena. 2012; 97(1): 71–84.
37. Hong H. Assessing landslide susceptibility based on hybrid Best-first decision tree with ensemble learning model. Ecol. Indic. 2023; 147:109968.
38. Hunter G., Fell R. Travel distance angle for "rapid" landslides in constructed and natural soil slopes. Can. Geotech. J. 2003; 40(6): 1123–1141.
39. Donati L., Turrini M.C. An objective method to rank the importance of the factors predisposing to landslides with the GIS methodology: application to an area of the Apennines (Valnerina; Perugia, Italy). Eng. Geol. 2002; 63(3-4): 277–289.
40. Roback K., Clark M.K., West A.J., Zekkos D., Li G., Gallen S.F., Chamlagain D., Godt J.W. The size, distribution, and mobility of landslides caused by the 2015 Mw 7.8 Gorkha earthquake, Nepal. Geomorphology. 2017;301:121–138.
41. Kisi O., Parmar K. Application of least square support vector machine and multivariate adaptive regression spline models in long-term prediction of river water pollution. J. Hydrol. 2016; 534(1):104–112.
42. Zheng G., Yang P., Zhou H., Zeng C., Yang X., He X., Yu X. Evaluation of the earthquake induced uplift displacement of tunnels using multivariate adaptive regression splines. Comput. Geotech. 2019; 113(1):1–10.
43. Mohammady M. Badland erosion susceptibility mapping using machine learning data mining techniques, Firozkuh watershed, Iran. Nat. Hazard. 2023; 117(1):703–721.
44. Dlamini, W.M. Analysis of deforestation patterns and drivers in Swaziland using efficient Bayesian multivariate classifiers. Model. Earth Syst. Environ. 2016; 2(4): 1–14.
45. Mosaffaie J., Salehpour Jam A., Tabatabaei M.R. Comparing the Validity of Statistical and Knowledge-Based Methods for Landslide Susceptibility Mapping. J. Agric. Sci. Technol. 2024b; 26(3): 695-709.
46. Salehpour Jam A., Mosaffaie J., Sarfaraz F., Shadfar S., Akhtari R. GIS-based landslide susceptibility mapping using hybrid MCDM models. Nat. Hazard. 2021; 108(1):1025–1046.
47. Salehpour Jam A., Mosaffaie J., Tabatabaei M.R. Raster-based landslide susceptibility mapping using compensatory MADM methods. Environ. Model. Softw. 2023; 159: 105567.